

CHEM**BIO**CHEM

Supporting Information

© Copyright Wiley-VCH Verlag GmbH & Co. KGaA, 69451 Weinheim, 2008

Supporting Information

for

From Kinase to Cyclase: An Unusual Example of Catalytic Promiscuity Modulated by Metal Switching

Israel Sánchez-Moreno, Laura Iturrate, Rocío Martín-Hoyos, María Luisa Jimeno,
Montaña Mena, Agatha Bastida and Eduardo García-Junceda*

Contents

	Page
Materials and General Procedures	S2
Cloning, overexpression and purification of DHAK	S2
Protein analysis	S4
Enzyme activity assays	S4
Steady-state kinetic assays and inhibition studies	S6
NMR procedures	S9
NMR structural elucidation	S9
Molecular docking studies	S13
Sequence similarity searching and phylogenetic tree analysis	S13

Materials and General Procedures

SDS-PAGE was performed using 10% and 5% acrylamide in the resolving and stacking gels, respectively. Gels were stained with Coomassie brilliant blue R-250 (Applichem GmbH, Germany). Electrophoresis were always run under reducing conditions, in the presence of 5% β -mercaptoethanol. Protein and DNA gels were quantified by densitometry. Triosephosphate isomerase (TIM) and α -glycerophosphate dehydrogenase (α GDH), were purchased from Sigma-Aldrich (St. Louis, MO). Restriction enzymes, *Taq* polymerase and T4-DNA ligase were purchased from MBI Fermentas AB (Lithuania). *Citrobacter freundii* CECT 4626 was provided from the Spanish Type Culture Collection (CECT). *E. coli* BL21(DE3) competent cells were purchased from Stratagene Co. (San Diego, CA). PCR primers were purchased from Isogen Life Science (Spain) and the pRSET-A expression vector was purchased from Invitrogen Co. (Carlsbad, CA). Isopropyl- β -D-thiogalactopyranoside (IPTG) was purchased from Applichem GmbH (Germany). Plasmids and PCR purification kits were from Promega (Madison, WI) and DNA purification kit from agarose gels was from Eppendorf (Hamburg, Germany). Nickel-iminodiacetic acid (Ni^{2+} -IDA) agarose was supplied by Agarose Bead Technologies (Spain). All other chemicals were purchased from commercial sources as reagent grade.

Cloning, overexpression and purification of DHAK from C. freundii CECT 4626

DNA manipulation was according to standard procedures (Sambrook et al. 1989). DNA template for amplification of the *dhak* gene was obtained from the *Citrobacter freundii* strain CECT 4626. Primers for PCR amplification were designed based on the nucleotide sequence of the *dhak* gene from the strain DSM 30040 (GeneBank Accession N^o U09771). The oligonucleotides 5'-ATATTAAAGCTTCAAAACATTACT-CAG-3' and 5'-TATTACTCGAGTTACAGCCAGCGCACTGGC-3' were used as leftward and rightward primers respectively (the recognition sequence for HindIII and XhoI are underlined). PCR amplification was performed in a 100 μ L reaction mixture and subjected to 30 cycles of amplification. The cycle conditions were set as follows: denaturation at 94°C for 1 min, annealing at 55 °C for 1 min and elongation at 72 °C for 1.5 min. The purified PCR product was digested with XhoI and HindIII and ligated into the double digested vector pRSET-A to yield the plasmid pRSET-*dhak*. This plasmid was transformed into *E. coli* BL21(DE3) competent cells.

A colony containing the plasmid pRSET-*dhak* was cultured in Luria-Bertani (LB) broth containing ampicillin (250 µg/mL) at 37 °C with shaking. When the culture reached an OD₆₀₀ of 0.5-0.6, DHAK expression was induced with IPTG (1 mM) and the temperature was dropped to 30 °C. The culture was maintained O/N. After that, the culture was centrifuged at 10,000 x g during 10 min at 4 °C and the resulting pellet was treated with lysozyme and DNase for protein extraction.¹

The recombinant protein containing an N-terminal 6xHis tag was purified by IMAC in a Ni²⁺-IDA-agarose column pre-equilibrated with sodium phosphate buffer (20 mM, pH 7.5). DHAK was eluted with the same buffer containing imidazole 0.25 M. All the fractions containing protein were pooled together and further purified by size-exclusion chromatography on a HiLoad 26/60 Superdex 75 PG column controlled using the AKTA-FPLC system (GE Healthcare Life Science). The column was developed in 50 mM phosphate buffer pH 7.2 containing NaCl (0.15 M) at a constant flow rate of 1.0 mL/min (Figure S1).

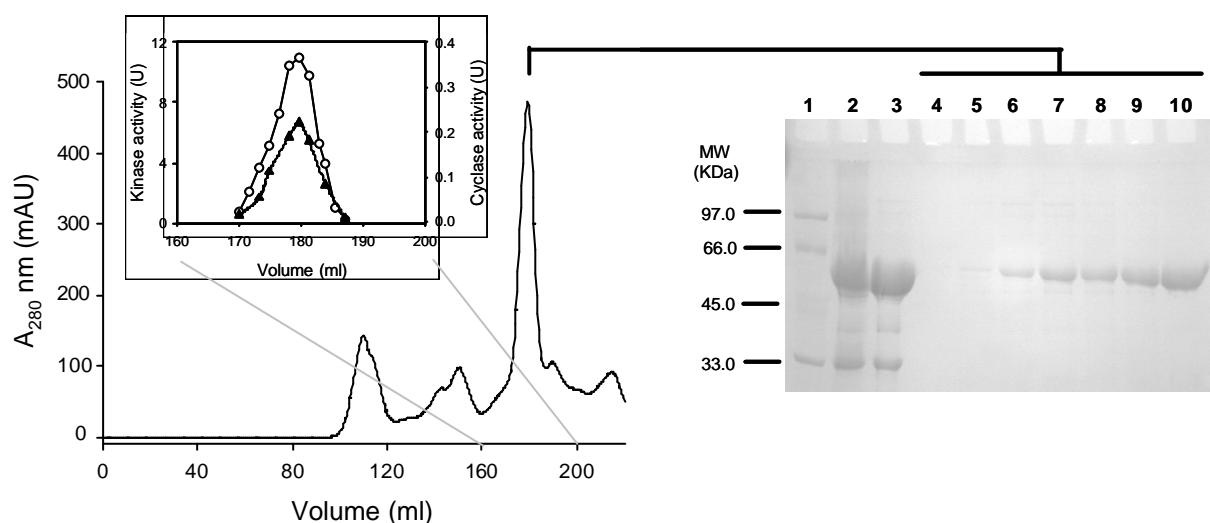


Figure S1. Purification of the recombinant DHAK. Chromatogram of the size-exclusion step. Insert shows the elution profile of both kinase (?) and cyclase (?) activities. SDS-PAGE shows: lane 1, low molecular weight markers; lane 2, cell free extract; lane 3, DHAK after IMAC step; lanes 4-10 fractions containing kinase and cyclase activities.

¹ A. Bastida, A. Fernández-Mayoralas, R. Gómez, F. Iradier, J. C. Carretero, E. García-Junceda, *Chem. Eur. J.* **2001**, 7, 2390–2397

Protein analysis

Amino acid analysis of purified DHAK aliquots was performed at the Department of Biochemistry and Molecular Biology of the Complutense University of Madrid to determine the protein concentration. The absorption spectrum of different quantified samples allowed determination of the molar extinction coefficient of DHAK at 280 nm ($\epsilon^{280} = 35998.84 \text{ M}^{-1} \cdot \text{cm}^{-1}$).

Peptide mass fingerprint analysis from the SDS-PAGE band corresponding to the putative recombinant DHAK was performed at the Proteomic Unit of the Spanish National Center of Biotechnology (Centro Nacional de Biotecnología, CSIC). Samples were digested with sequencing grade trypsin overnight at 37 °C. The analysis by MALDI-TOF mass spectrometry produces peptide mass fingerprints and the peptides observed can be collated and represented as a list of monoisotopic molecular weights. Data were collected in the m/z range of 800-3600. 29 peptides covering the major part of the amino acid sequence of the protein were identified (Figure S2). Almost all the predicted tryptic peptides with molecular masses falling in the analyzed m/z range were found in the peptide mass fingerprint of the recombinant DHAK. Peptide mass fingerprinting verified that purified protein had the expected features of DHAK from *C. freundii* CECT 4626.

Enzyme activity assays

Phosphorylation of DHA was measured spectrophotometrically in a coupled enzymatic assay based in the reduction of DHAP to α -glycerophosphate, catalyzed by α GDH with concomitant oxidation of NADH to NAD^+ . The assays were run at 25 or 37 °C following the decrease of absorbance at 340 nm ($\epsilon_{\text{NADH}}^{340} = 6220 \text{ cm}^{-1} \cdot \text{M}^{-1}$) for 10 min in reaction mixtures of 1 mL containing Tris-HCl (40 mM, pH 8.0), DHA (2.5 μmol), NADH (0.2 μmol), ATP (5.0 μmol), MgSO_4 (5.0 μmol), α GDH (1.26 U), TIM (12.6 U) and DHAK. One unit of kinase activity was defined as the amount that produces 1 μmol of DHAP per min under the above conditions.



Figure S2. Peptide mass fingerprint of DHAK from *C. freundii* CECT 4626. Sequence of DHAK, indicating the theoretical trypsin cleavage sites (↓). The sequence of the identified peptides are shaded and underlined when overlapping. Molecular mass of each peptide is indicated in Da. Bold-inverted cells indicate the modified aminoacid with respect to the sequence of the protein from the strain DSM 30040.

FMN cyclase activity was determined by measuring the formation of 4',5'-cFMN from FAD by HPLC with $A_{430\text{nm}}$ monitoring in reaction mixtures of 1 mL containing Tris-HCl (40 mM, pH 7.5), MnCl_2 (12 mM), FAD (0.25 mM) and DHAK. Full reaction mixtures were incubated from 10 to 60 min. HPLC was performed in an Inertsil ODS-2 column following the previously described assay with minor modifications.² The mobile phase employed was 20 mM sodium phosphate, pH 6.0, and methanol at a final concentration of 35% (v/v) and the chromatography was run under isocratic conditions at 1 mL/min flow rate (Figure S3). One unit of cyclase activity was defined as the amount of enzyme that produces 1 μmol of 4',5'-cFMN per min under the above conditions.

²F. J. Fraiz, R. M. Pinto, M. J. Costas, M. Ávalos, J. Canales, A. Cabezas, J. C. Cameselle, *Biochem. J.* **1998**, 330: 881-888.

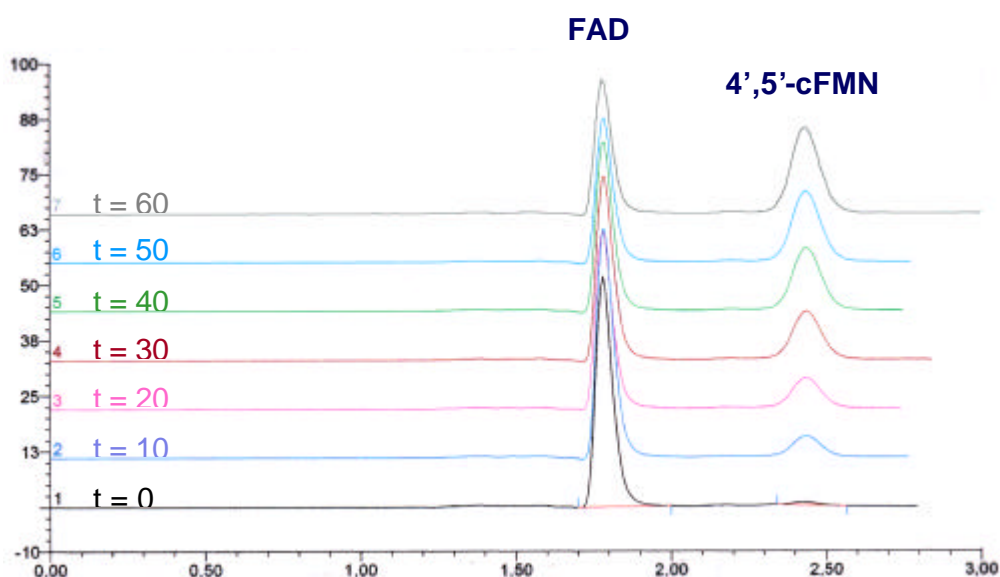


Figure S3. HPLC chromatograms of the cyclization reaction catalysed by the DHAK from *C. freundii* strain CECT 4626.

Steady-state kinetic assays and inhibition studies

Steady-state kinetic assays for kinase activity were measured at 25 °C in 96-well plates in a total volume of 0.3 mL. Measurements of kinetic parameters for DHA were performed with 0.08 µg/mL of purified DHAK at 10 different DHA concentrations and with saturating concentration of $[\text{MgATP}]^{2-}$ (5.0 mM; Figure S4A). Assays to determine the kinetic parameters for $[\text{MgATP}]^{2-}$ complex were performed with 1.0 µg/mL of purified DHAK at sixteen concentrations of complex using a constant Mg^{2+} excess of 40 mM and 2.5 mM of DHA (Figure S4C). Assays to determine the kinetic parameters for $[\text{MnATP}]$ were performed with 0.9 µg/mL of purified DHAK at 12 concentrations of complex using 2.5 mM of DHA (Figure S4D). In order to avoid Mn^{2+} excess inhibition (see Figure 2) the maximum MnCl_2 concentration used was 1.3 mM (7.5 fold lower than ATP concentrations in each kinetic point). Cyclase activity was measured at 7 FAD concentrations in presence of MnCl_2 (12 mM) using 4.1 µg/mL of purified DHAK in 25 °C kinetic (Figure S4B) and 1.7 µg/mL of enzyme in 37 °C kinetic.

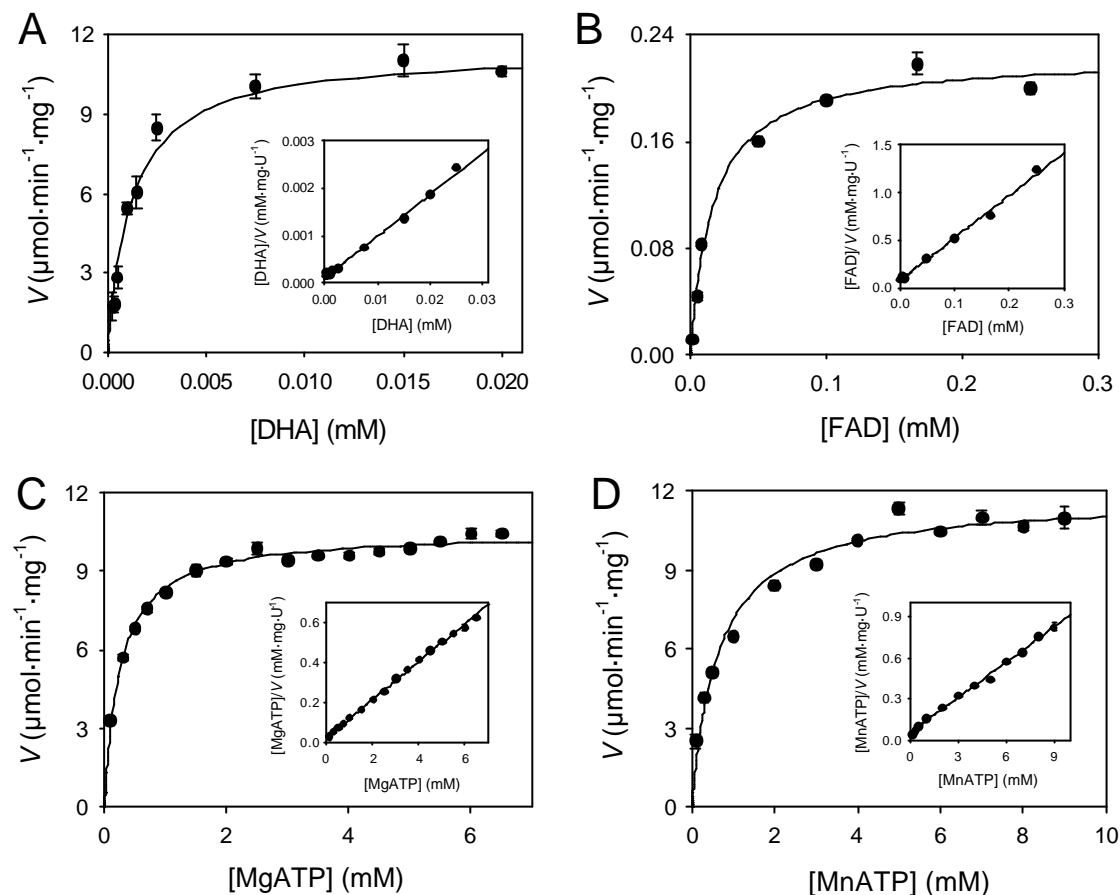


Figure S4. Substrate kinetics of kinase and cyclase activity for DHAK from *C. freundii* CECT 4626 at 25°C. Kinase activity of purified DHAK was measured at several concentrations of DHA (A), MgATP (C) and MnATP (D) maintaining constant excesses of MgATP (A) and DHA (C and D). Cyclase activity of purified DHAK was measured at various FAD concentrations in presence of MnCl_2 12 mM. The inserts show Hanes-Woolf plots used for kinetic constants determination.

Kinetic constants were obtained using the built-in nonlinear regression tools in SigmaPlot 8.0 and by nonlinear regression to the experimental data using the SIMFIT package³ (url: <http://www.simfit.man.ac.uk>).

Inhibition studies were conducted in steady-state kinetic assays for FAD, $[\text{MgATP}]^2$ and $[\text{MnATP}]$ in presence of several concentrations of considered inhibitor (Figure S5). Inhibition of cyclase activity by ATP (Figure S5A), DHA (Figure S5B) and AMP (Figure S5C) were analyzed in FAD activity assays in presence of increasing concen-

³ H. G. Holzhütter, A. Colosimo, *Bioinformatics* **1989**, 6, 23-28.

trations of inhibitor. Inhibition of kinase activity by AMP was analyzed using $[\text{MgATP}]^{2-}$ (Figure S5D) and $[\text{MnATP}]$ (Figure S5E) as phosphate donors. Inhibition of kinase activity by FAD was analyzed in $[\text{MnATP}]$ kinetic with increasing concentrations of inhibitor by linear regression to Hanes-Woolf plots. (Figure 3A). The secondary plots $[\text{FAD}]$ versus V_{max}/K_M and $[\text{FAD}]$ versus $1/V_{\text{max}}$ were used to calculate k_{iu} and k_{ic} respectively (Figure 3B and C). FAD concentrations over 0.7 could not be used due to the high absorption of the inhibitor at 340 nm, that made impossible to take accurate data.

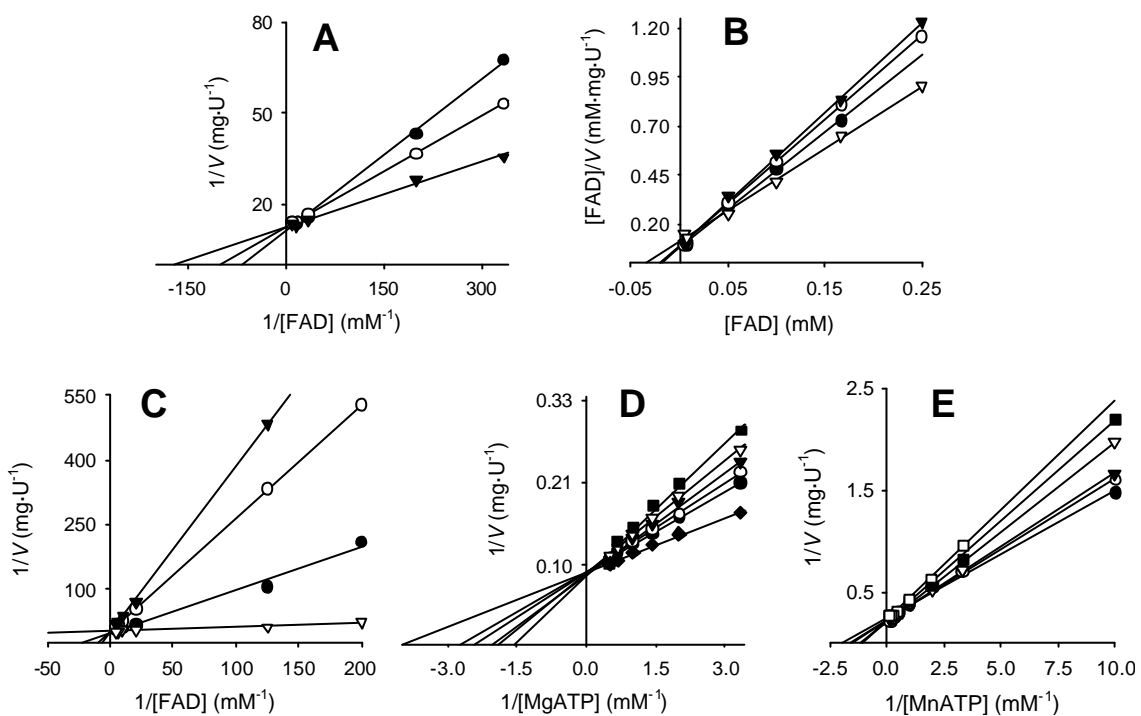


Figure S5. Inhibition kinetics for DHAK from *C. freundii* CECT 4626. A) Lineweaver-Burk plots from cyclase activity at different concentrations of FAD in presence of increasing concentrations of ATP: 30 (?), 100 (?) and 150 nM (?). B) Hanes-Woolf plots from cyclase activity at different concentrations of FAD in presence of increasing concentrations of DHA: 0 (∇), 50 (?), 100 (?) and 200 mM (?). C) Lineweaver-Burk plots from cyclase activity at different concentrations of FAD in presence of increasing concentrations of AMP: 0 (∇), 0.5 (?), 2.5 (?) and 5.0 mM (?). D) Lineweaver-Burk plots from kinase activity at different concentrations of MgATP and constant excess of DHA, in presence of increasing concentrations of AMP: 0 (?), 3 (?), 6 (?), 9 (?), 12 (∇) and 15 mM (\dagger). E) Lineweaver-Burk plots from kinase activity at different concentrations of MnATP and constant excess of DHA, in presence of increasing concentrations of AMP: 5 (?), 10 (?), 15 (?), 20 (∇), 25 (\dagger) and 30 mM (?).

NMR procedures

^1H and ^{13}C NMR spectra, using D_2O as solvent, were recorded on a Varian SYSTEM 500 spectrometer equipped with a 5 mm HCN cold probe with field z-gradient, operating at 500.13 and 125.76 MHz for ^1H and ^{13}C , respectively. ^{31}P NMR spectrum was recorded on a Varian Mercury 400 operating at 161.9 MHz. The sample temperature was maintained constant at 298 K. 1D NMR experiments were performed by using standard Varian pulse sequences. 2D [^1H , ^1H] NMR experiments (gCOSY and TOCSY) were carried out with the following parameters: a delay time of 1 s, a spectral width of 3000 Hz in both dimensions, 4096 complex points in t_2 and 4 transients for each of 256 time increments, and linear prediction to 512. The data were zero-filled to 4096×4096 real points. 2D [^1H , ^{13}C] NMR experiments (gHSQC and gHMBC) used the same ^1H spectral window, a ^{13}C spectral windows of 15 000 Hz, 1 s of relaxation delay, 1024 data points, and 256 time increments, with a linear prediction to 512. The data were zero-filled to 4096×4096 real points. Typical numbers of transients per increment were 4 and 16, respectively.

NMR structural elucidation

Unequivocal structural elucidation of the purified product was carried out by the combined use of 1D and 2D [^1H , ^1H] and [^1H , ^{13}C] NMR experiments (gCOSY, TOCSY, gHSQC and gHMBC). The ^1H and ^{13}C 1D NMR spectra showed chemical shifts that were consistent with a mixture of two compounds in a ratio 4:1 (Figures S7 and S8). The major compound was identified as riboflavin 4'-5' phosphate (cFMN). The assignment of the 7,8-dimethylisoalloxazine moiety was based on 1D ^1H NMR and 2D gHSQC and gHMBC. Using the C11 resonance as the starting point, the assignments of all protons and carbons of the ribityl chain were obtained easily from gCOSY, gHSQC and gHMBC experiments (Figure S6). The structure of cFMN was supported by ^{31}P -NMR measurements, which showed a narrow signal at a chemical shift of 19.20 p.p.m. (relative to 85% orthophosphoric acid) which must be due to cFMN, close to a much broader signal (-5 to 10 p.p.m.) due to the buffer phosphate (Figure S9). The presence of a measurable $^3J(^{31}\text{P}, ^{13}\text{C})$ coupling constant for C3' indicated the existence of a cyclic phosphate fragment. NMR relevant data are collected in Table S1 showing a good concordance with those published for cFMN.

Finally, the structure elucidation of the minor compound was carried out. Two aromatic singlets at 8.00 and 8.12 ppm and an anomeric doublet at 5.84 ppm were ob-

served in the ^1H spectrum. Only sugar carbons were observed in the 1D ^{13}C spectrum. However, from gCOSY, gHSQC and gHMBC experiments (Figure S6B) the assignment of NMR spectra was possible (Table S1). So, the minor compound was identified as adenosine 5'-phosphate (AMP).

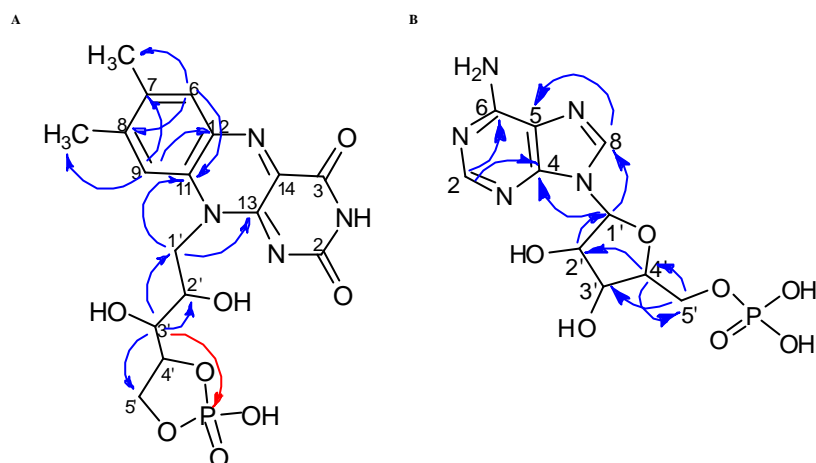


Figure S6. Relevant observed [^1H - ^{13}C] gHMBC correlations (blue) and [^1H - ^{31}P] gHMBC (red) for major and minor compounds. **A:** Riboflavin 4'-5' phosphate (cFMN). **B:** Adenosine mono-phosphate (AMP).

Table S1. ^1H and ^{13}C NMR relevant data (*d*, ppm) in D_2O .

cFMN			AMP		
Position	$d^{13}\text{C}$	$d^1\text{H}$	Position	$d^{13}\text{C}$	$d^1\text{H}$
<i>7,8-dimethylisalloxazine</i>			<i>Adenine</i>		
2	157.8		2		8.00
4	161.0		4	148.1	
6	130.2	7.46	5	119.1	
7	139.3		6	155.6	
8	150.6		8	140.9	8.12
9	116.7	7.57			
11	131.4				
12	134.2				
13	149.8				
14	133.8				
$\text{CH}_3(\text{C}7)$	18.8	2.22			
$\text{CH}_3(\text{C}8)$	20.7	2.37			

<i>Ribityl Chain</i>			<i>Ribose</i>		
1'	47.6	4.58	1'	88.2	5.84
		4.90			
2'	69.3	4.12	2'	73.7	4.56
3'	72.5	3.97	3'	70.5	4.25
4'	75.2	4.56	4'	85.7	4.11
5'	66.3	4.16	5'	61.4	3.74
		4.30			3.66

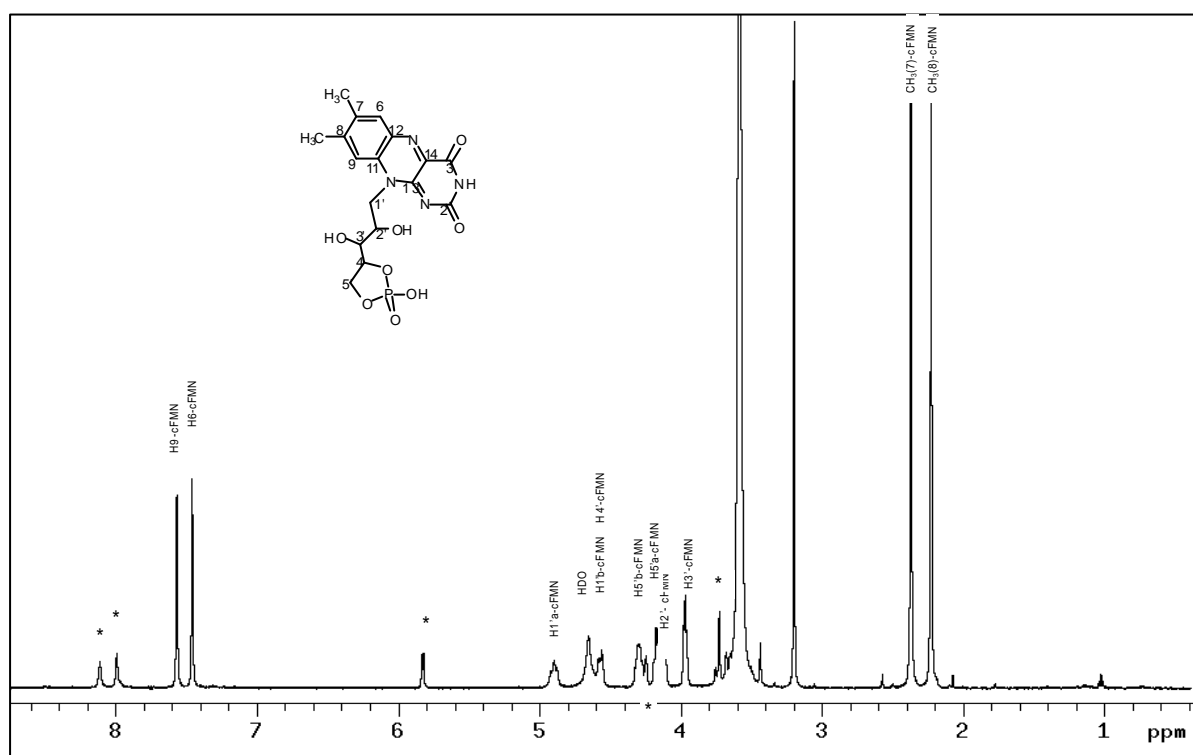


Figure S7 ^1H NMR (500MHz, D_2O) spectrum of riboflavin 4'-5' phosphate (cFMN). * Minor component resonances.

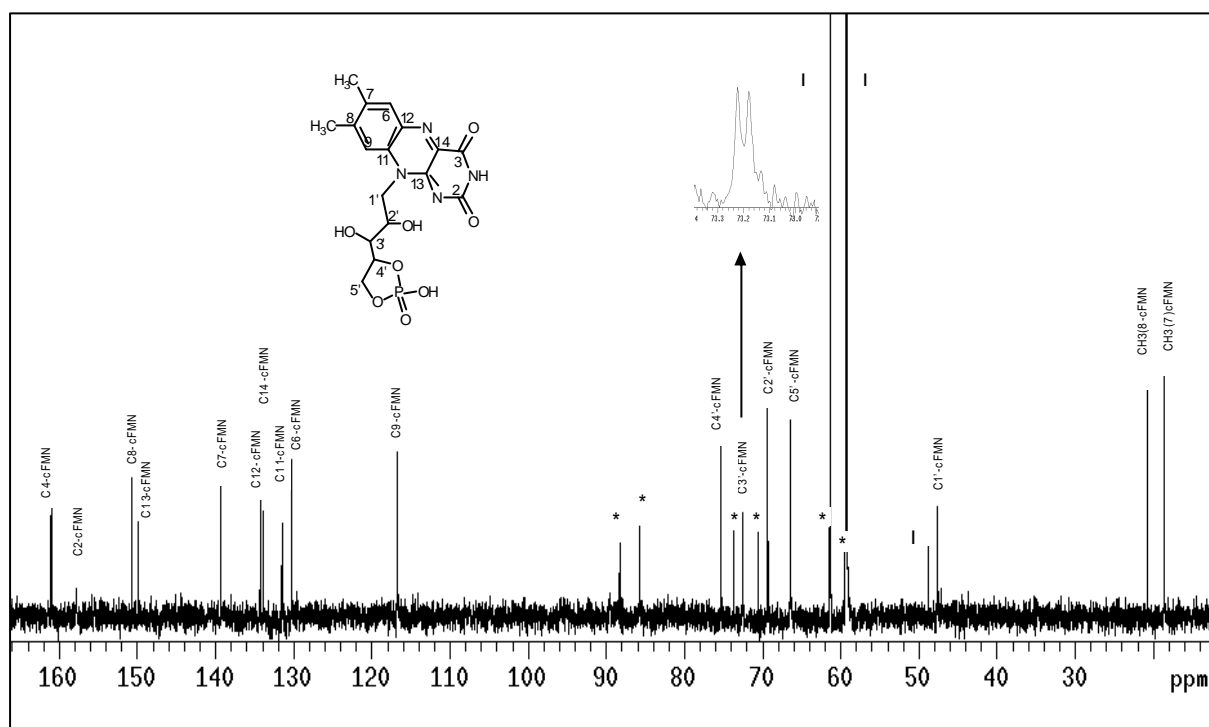


Figure S8 ^{13}C NMR (125MHz, D_2O) spectrum of riboflavin 4'-5' phosphate (cFMN).

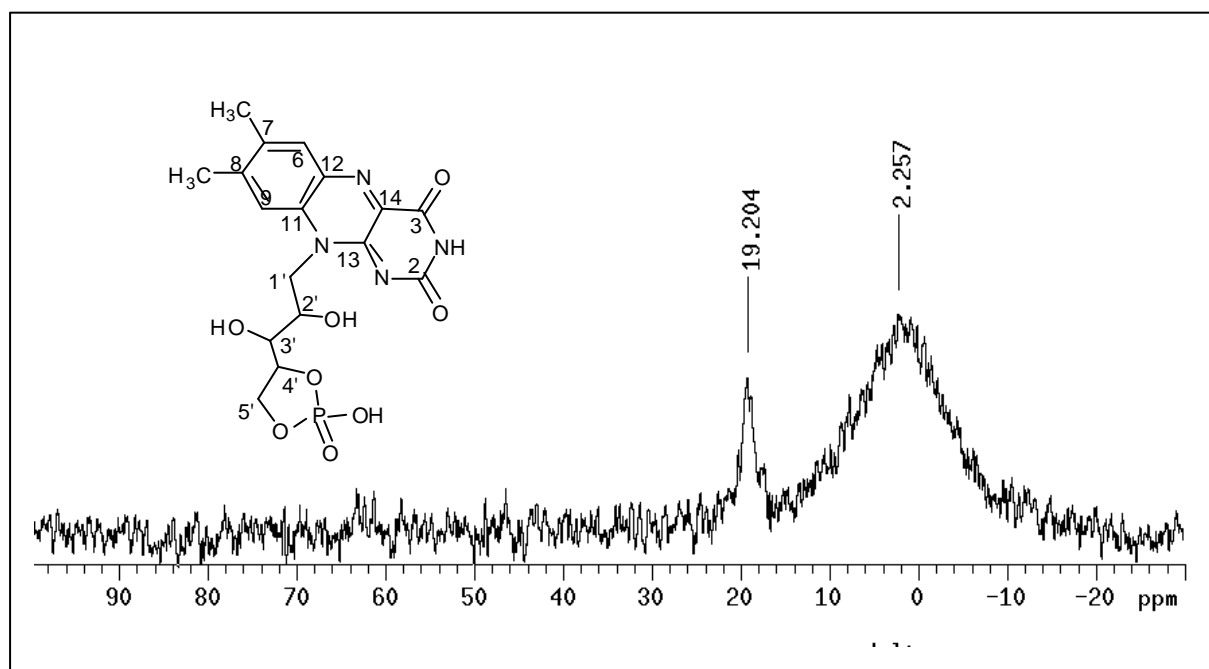


Figure S9 ^{31}P NMR (161.9 MHz, D_2O) spectrum of riboflavin 4'-5' phosphate (cFMN)

Molecular docking studies

Docking simulation was conducted with AutoDock 3.0.4⁴ which is a fully automated docking suited of programs, which employs a genetic algorithm (GA) as a search engine. The coordinates of the protein (1un9)⁵ were taken from the Protein Data Bank. Before docking, compounds were minimised by Molecular mechanics (PM3) using MM3* force fields. Protein was prepared by eliminating heteroatoms and adding the hydrogen atoms (polar only). Polar hydrogen atoms and Gasteier-Huckel were added to the compounds by using the auxiliary program AutoDock Tools (ADT). Energies were evaluated from recalculated potentials grids with molecular affinity potentials. Affinity grid files were generated using the auxiliary program Autogrid. The centers of the coordinates of the ligands were taken as the centers of the grids, and the dimensions of the grids were 76/63/123 for the FAD with points separated by 0.37 Å. After docking, the 50 solutions were clustered into groups with RMS deviations of 1 Å. The FAD conformers were bound to the ATP-binding domain of the enzyme (L-domain; Figure S10). The optimal docked conformer was to the global minimum giving docked energy of -5.38 Kcal/mol

Sequence similarity searching and phylogenetic tree analysis

A similarity search for the DHAK from *C. freundii* CECT 4626 (GeneBank Accession N° DQ473522) was performed by BLASTP⁶ on the NCBI non-redundant SwissProt database using default settings. 30 proteins sequences with significant similarity were identified and analysed by BLAST pairwise alignment. The 17 proteins showing a maximum sequence differences below 0.75 were considered to build a matrix of distance according to the Kimura method.⁷ Subsequently, the unrooted tree was derived by the Fast Minimum Evolution method,⁸ as implemented at the NCBI server.

⁴ G. M. Morris, D. S. Goodsell, R. S. Halliday, R. Huey, W. E. Hart, R. K. Belew, A. J. Olson, *J. Comput. Chem.* **1998**, 19, 1639-1662.

⁵ C. Siebold, I. Arnold, L. F. García-Alles, U. Baumann, B. Erni, *J. Biol. Chem.* **2003**, 278, 48236-48244.

⁶ a) S. F. Altschul, T. L. Madden, A. A. Schäffer, J. Zhang, Z. Zhang, W. Miller, D. J. Lipman *Nucleic Acids Res.* **1997**, 25, 3389-3402; b) S. F. Altschul, J. C. Wootton, E. M. Gertz, R. Agarwala, A. Morgulis, A. A. Schäffer, Y.-K. Yu *FEBS J.* **2005**, 272, 5101-5109.

⁷ M. Kimura, *J. Mol. Evol.* **1980**, 16, 111-120.

⁸ R. Desper, O. Gascuel, *J. Comput. Biol.* **2002**, 9, 687-705.

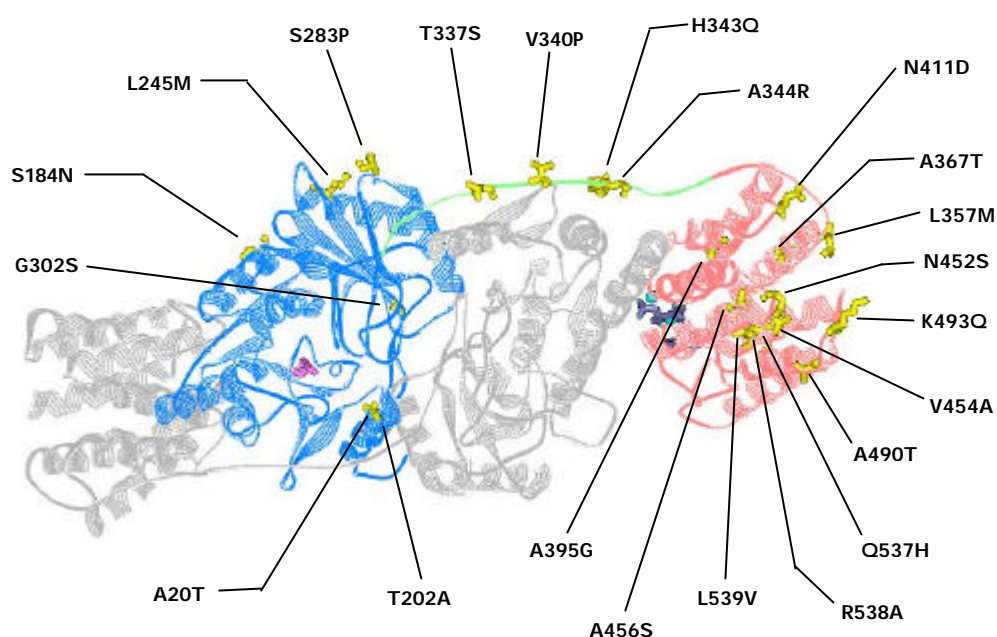


Figure S10. 3D structure of the dimeric DHAK from *C. freundii* DSM 30040.⁴ In the N-terminal domain —K-domain (blue)— is where the DHA (purple) binding site is located. The ATP (dark blue) binding site is found in the C-terminal —L-domain (pink). In yellow are shown the amino acids in which differ the DSM 30040 isoform from the CECT 4626 isoform.